Liquid Crystals
Publication details, including instructions for authors and subscription information:
http://www.informaworld.com/smpp/title~content=t713926090

Liquid crystalline molecules with hydrogen-bonding networks in the direction of molecular short axes

Shigeo Kohmoto[a]; Yasunobu Someya[a]; Keiki Kishikawa[a]
[a] Department of Applied Chemistry and Biotechnology, Graduate School of Engineering, Chiba University, Inage-ku, Chiba, Japan

To cite this Article Kohmoto, Shigeo , Someya, Yasunobu and Kishikawa, Keiki(2010) 'Liquid crystalline molecules with hydrogen-bonding networks in the direction of molecular short axes', Liquid Crystals, 37: 2, 209 — 216
To link to this Article: DOI: 10.1080/02678290903495012
URL: http://dx.doi.org/10.1080/02678290903495012

Liquid Crystals,
Vol. 37, No. 2, February 2010, 209–216

Taylor & Francis
Taylor & Francis Group

Liquid crystalline molecules with hydrogen-bonding networks in the direction of molecular short axes

Shigeo Kohmoto*, Yasunobu Someya and Keiki Kishikawa

Department of Applied Chemistry and Biotechnology, Graduate School of Engineering, Chiba University, 1-33 Yayoi-cho, Inage-ku, Chiba 263-8522, Japan

(Received 29 September 2009; final version received 17 November 2009)

The salts of 4-alkoxy-3,5-bis(hydroxymethyl)benzoic acids and alkylamine give stable smectic liquid crystals in a wide temperature range. These smectic phases were investigated by polarised optical microscopy, differential scanning calorimetry and powder X-ray diffraction. An inter-digitated structure of the plough-shaped network created by the inter-molecular hydrogen bonding between the hydroxymethyl groups in the direction of the molecular short axis is proposed.

Keywords: carboxylic acid-amine salts; hydrogen bonding; supramolecular liquid crystals

1. Introduction

Self-organised materials are assembled with the aid of non-covalent bonds, such as hydrogen bonds, ionic bonds and coordination bonds [1–7]. These interactions are essential to organise highly ordered superstructures. In liquid crystals, these bonds contribute to create rigid cores [8–16] and stable side chains [11–13, 17, 18] in both calamitic and disk-like molecules. In rod-like molecules, hydrogen bonding networks are usually constructed in the direction of molecular long axes [19–22]. In contrast, examples of hydrogen bonding networks in the direction of molecular short axes were very limited [23–27]. Generally, efficient rotational fluctuations of liquid crystalline molecules along molecular long axes are highly demanded for stable mesophase formation. Therefore, multiple hydrogen bondings in the direction of molecular short axes are unfavourable due to the prevention of the required rotational fluctuations (Figure 1).

Moreover, the addition of the hydrogen bonding sites disturbs the core–core interaction due to the elongation of the distance between the adjacent cores. As a result, the destabilisation of the mesophase occurs to give the corresponding crystals. Our question is: does this disturbance of rotational fluctuations really destabilise the resulting mesophase? Rather, can it stabilise the mesophase under certain conditions? The advantage of the creation of a hydrogen-bonding network is to segregate efficiently the hydrogen-bonded rigid cores from the flexible alkyl chain parts. Especially for the ionic cores, this segregation contributes to the stabilisation of the mesophase.

For this purpose, we prepared 4-alkoxy-3,5-bis(hydroxymethyl)benzoic acids **1** which have three interactive sites, two hydroxyl groups and a carboxyl group (Scheme 1). The benzoic acids **1** are expected to assemble by hydrogen bonding between the hydroxymethyl groups in the direction of molecular short axes. The remaining carboxylic acid moiety can form salts in the direction of molecular long axis by an acid–base interaction when amines are added. The salt formation results in the supramolecular assembly to segregate between hydrophilic and hydrophobic moieties [11, 28–30]. Ionic interactions could also reinforce the liquid crystallinity of **1**. Herein, we present a novel example of rod-like molecules capable of showing liquid crystallinity even though they possess hydrogen-bonding sites on both sides of the core toward the direction of the molecular short axes.

2. Experimental

2.1 General methods and materials

^{1}H NMR (nuclear magnetic resonance) and ^{13}C NMR spectra were recorded on JNM-LA400s and LA500 spectrometers. Chemical shifts are reported in parts per million (ppm) with the signals of TMS for ^{1}H NMR spectra and solvents for ^{13}C NMR spectra used as internal standards. Infrared (IR) spectra were recorded on a JASCO FT/IR410 spectrometer. High-resolution mass spectra were recorded using a JEOL JMS-HX100 instrument. Thermal transitions of the ionic complexes were investigated by differential scanning calorimetry (DSC) using a MAC Science DSC3100S differential scanning calorimeter and heating and cooling rates of 5°C min^{-1}. Using a Nikon Eclipse E400POL equipped with an Instec HCS400 hot stage, polarising optical microscopy (POM) was

---

*Corresponding author. Email: kohmoto@faculty.chiba-u.jp

ISSN 0267-8292 print/ISSN 1366-5855 online

DOI: 10.1080/02678290903495012
http://www.informaworld.com

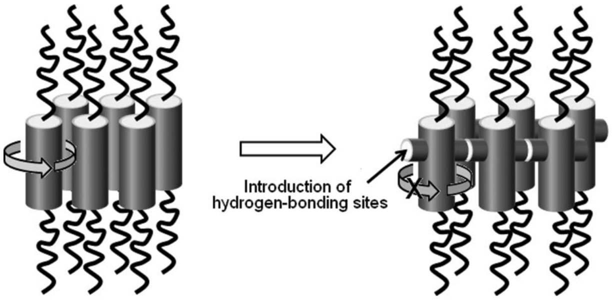

Figure 1. Prevention of the spinning of liquid crystal molecules by the hydrogen-bonding network in the direction of molecular short axes.

used to verify thermal transitions and characterise anisotropic textures. X-ray diffraction (XRD) experiments were performed with Cu K_α radiation by using a Rigaku RINT 2200 diffractometer. All commercially available chemicals and solvents were of reagent grade and used as received without further purification.

2.2 Synthesis

*2.2.1 Ethyl 4-hexoxy-3,5-bis(hydroxymethyl) benzoate, (**3a**)*

Compound **2** (0.401 g, 1.77 mmol), potassium carbonate (0.361 g, 2.61 mmol), and potassium iodide (0.273 g, 1.64 mmol) were dissolved in acetone (100 ml) and stirred for 30 min. Then, 1-bromohexane (0.506 g, 3.07 mmol) was added to the solution and the resulting mixture was stirred under reflux for 2 days. After filtering off the precipitate formed, the solvent was evaporated. The residue was purified with column chromatography on silica gel (hexane/ethyl acetate = 2:1) to give **3a** as a colourless crystal (0.383 g, 70%). Mp 79–80°C: ^{1}H NMR (400 MHz, $CDCl_3$) δ 0.92 (t, J = 7.1, 3H), 1.33–1.41 (m, 7H), 1.49 (quintet, J = 7.6, 2H), 1.83 (quintet, J = 7.2, 2H), 3.94 (t, J = 6.8, 2H), 4.36 (q, J = 7.2, 2H), 4.75 (s, 4H), 8.04 (s, 2H): ^{13}C NMR (100 MHz, $CDCl_3$) δ 14.1, 14.4, 22.6, 25.7, 30.4, 31.7, 60.8, 61.1, 75.4, 126.6, 130.3, 134.3, 159.1, 166.1: MS (FAB) *m*/*z* 311 $[MH]^+$, 333 $[M{+}Na]^+$: IR (KBr) ν 1715 cm^{-1} (C=O): Anal. calc. for $C_{17}H_{26}O_5$: C, 65.78; H, 8.44. Found: C, 65.78; H, 8.31.

*2.2.2 Ethyl 4-dodecyloxy-3,5-bis(hydroxymethyl) benzoate, (**3b**)*

Compound **2** (0.997 g, 0.441 mmol), potassium tertiarybutoxide (0.502 g, 4.47 mmol), and potassium iodide (0.075 g, 0.453 mmol) were dissolved in *N,N*-dimethylformamide (20 ml) and stirred for 30 min. After the addition of 1-bromododecane (1.0 ml, 4.2 mmol), the solution was stirred for ca. 2 days at 70°C. The resulting solution was neutralised with an aqueous solution of HCl (1M) and extracted with ethyl acetate. The organic layer was dried over anhydrous magnesium sulphate, and the solution was evaporated. The residue was purified with column chromatography on silica gel (hexane/ethyl acetate = 2:1) to give **3b** as a colourless crystal (1.35 g, 77 %). Mp 69–70.5°C: ^{1}H NMR ($CDCl_3$, 500 MHz) δ 0.88 (t, J = 6.9, 3H), 1.27-1.48 (m, 21H), 1.81 (quintet, J = 7.1, 2H), 3.92 (t, J = 6.6, 2H), 4.35 (q, J = 7.2, 2H), 4.73 (s, 4H), 8.01 (s, 2H): ^{13}C NMR ($CDCl_3$, 125.6 MHz) δ 14.1, 14.4, 22.7, 26.0, 29.4, 29.5, 29.58, 29.62, 29.65, 29.67, 30.4, 31.9, 60.7, 61.1, 75.4, 126.5, 130.2, 134.4, 159.0, 166.2: MS (FAB) *m*/*z* 395 $[MH]^+$, 417 $[M{+}Na]^+$: IR (KBr) ν 1711 cm^{-1} (C=O): Anal. calc. for $C_{23}H_{38}O_5$: C, 70.02; H, 9.71. Found: C, 70.29; H, 9.65.

*2.2.3 Ethyl 4-octadecyloxy-3,5-bis(hydroxymethyl) benzoate, (**3c**)*

In a similar manner as for the synthesis of **3b**, compound **3c** was prepared by *O*-alkylation of **2** with 1-bromooctadecane in 39% yield as a white powder. Mp 86–89°C: ^{1}H NMR ($CDCl_3$, 500 MHz) δ 0.88 (t, J = 7.0, 3H), 1.26–1.40 (m, 31H), 1.47 (quintet, J = 7.4, 2H) 1.81 (quintet, J = 7.2, 2H), 3.92 (t, J = 6.7, 2H), 4.35 (q, J = 7.1, 2H), 4.73 (s, 4H), 8.01 (s, 2H): ^{13}C NMR ($CDCl_3$, 125.6 MHz) δ 14.1, 14.4, 22.7, 26.0, 29.4, 29.5, 29.60, 29.64 29.68, 29.70, 29.73, 30.4, 31.9, 60.7, 61.1, 75.4, 126.5, 130.2, 134.3, 159.0, 166.2: MS

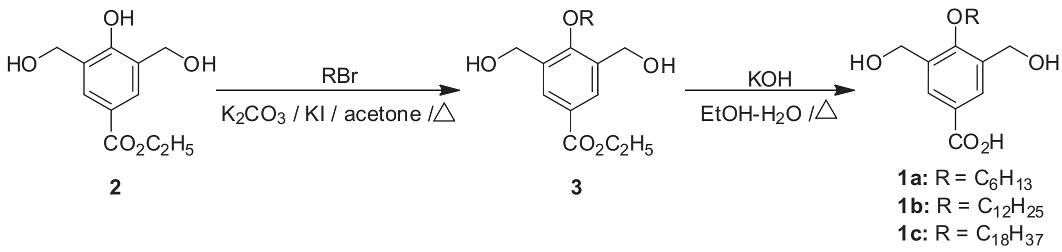

Scheme 1. Synthesis of bishydroxymethyl benzoic acid derivatives.

(FAB) *m*/*z* 480 [M+2H]$^+$, 502 [MH+Na]$^+$: IR (KBr) ν 1711 cm^{-1} (C=O): Anal. calc. for $C_{29}H_{50}O_5$: C, 72.76; H, 10.53. Found: C, 72.70; H, 10.16.

*2.2.4 4-Hexyloxy-3,5-bis(hydroxymethyl)benzoic acid, (**1a**)*

To an ethanol (20 ml) solution of **3a** (0.275 g, 0.886 mmol), an aqueous solution of KOH (15%, 2 ml) was added and stirred for 2 h at 70°C. After cooling to room temperature, the reaction mixture was neutralised with 1N HCl aqueous solution. The white powder precipitated was washed with H_2O. The crude product was reprecipitated with THF/hexane to give **1a** as a white powder (0.189 g, 76%). Mp 155–159°C: ^{1}H NMR (400 MHz, DMSO-d_6) δ 0.88 (t, $J = 6.8$, 3H), 1.31 (m, 4H), 1.42 (m, 2H), 1.69 (quintet, $J = 6.9$, 2H), 3.79 (t, $J = 6.4$, 2H), 4.54 (s, 4H), 7.95 (s, 2H): ^{13}C NMR (100 MHz, DMSO-d_6) δ 14.0, 22.1, 25.1, 29.8, 31.1, 57.6, 73.8, 125.9, 128.2, 135.3, 156.9, 167.3: MS (FAB) *m*/*z* 283 [MH]$^+$, 305 [M+Na]$^+$: IR (KBr) ν 1685 cm^{-1} (C=O): Anal. calc. for $C_{15}H_{22}O_5$: C, 63.81; H, 7.85. Found: C, 63.74; H, 7.72.

*2.2.5 4-Dodecyloxy-3,5-bis(hydroxymethyl)benzoic acid, (**1b**)*

In a similar manner as for the synthesis of **1a**, compound **1b** was prepared by hydrolysis of **3b** in 89% yield as a white powder. Mp 129–132°C: ^{1}H NMR (400 MHz, DMSO-d_6) δ 0.84 (t, $J = 6.8$, 3H), 1.23-1.33 (m, 16H), 1.42 (quintet, $J = 7.0$, 2H), 1.69 (quintet, $J = 6.9$, 2H), 3.79 (t, $J = 6.4$, 2H), 4.53 (s, 4H), 7.95 (s, 2H): ^{13}C NMR (100 MHz, DMSO-d_6) δ 13.9, 22.1, 25.4, 28.7, 28.8, 29.00, 29.03, 29.8, 31.3, 57.6, 73.7, 126.0, 128.2, 135.2, 156.8, 167.3: MS (FAB) *m*/*z* 367 [MH]$^+$, 389 [M+Na]$^+$: IR (KBr) ν 1710 cm^{-1} (C=O): HRMS (FAB) molecular weight calc. for $C_{21}H_{34}O_5$: *m*/*z* 367.2484 (MH$^+$). Found: 367.2453.

*2.2.6 4-Octadecyloxy-3,5-bis(hydroxymethyl) benzoic acid, (**1c**)*

In a similar manner as for the synthesis of **1a**, compound **1c** was prepared by hydrolysis of **3c** in 80% yield as a white powder. ^{1}H NMR (500 MHz, DMSO-d_6) δ 0.85 (t, $J = 6.6$, 3H), 1.23-1.26 (m, 28H), 1.43 (quintet, $J = 7.2$, 2H), 1.70 (quintet, $J = 6.9$, 2H), 3.79 (t, $J = 6.4$, 2H), 4.54 (s, 4H), 7.96 (s, 2H): ^{13}C NMR (125.6 MHz, DMSO-d_6) δ 13.9, 22.1, 25.4, 28.7, 28.9, 29.0, 29.8, 31.3, 57.6, 73.8, 125.9, 128.2, 135.2, 156.9, 167.3: MS (FAB) *m*/*z* 451 [MH]$^+$, 473 [M+Na]$^+$: IR (KBr) ν 1710 cm^{-1} (C=O): Anal. calc. for $C_{27}H_{46}O_5$: C, 71.96; H, 10.29. Found: C, 71.70; H, 10.18.

3. Results and discussion

3.1 Liquid crystallinity of 1

The phase transition behaviours of **1** are shown in Table 1. Only the compound with the longest alkyl chain **1c** showed a smectic A (SmA) liquid crystal phase in a narrow and a relatively wide temperature range on heating and on cooling, respectively. This SmA phase was observed as a dark region by POM because of the perpendicular molecular arrangement. Figure 2 shows its XRD pattern and DSC diagram. The layer distance observed by XRD was 37.6 Å at 134°C which was longer than the molecular length (28.7 Å). The results indicated that the carboxylic acid dimer was responsible for the layer distance. Rather short layer distance for the dimer might be originated in the interdigitation of the alkyl chains. A broad halo centred around 24–25° of 2θ indicates that this broad halo centre is of something involving another order of molecules other than the molten alkyl chains, as the layer distance deduced from it is rather short as a diameter for molten alkyl chains. The halo is assumed to be the overlap of those of stacking of phenyl rings and molten alkyl chains. The DSC of **1c** showed slight decrease of phase transition temperatures in both heating and cooling cycles gradually with increasing number of heating–cooling cycles (see the supplementary material Figure S1, which is available via the multimedia link on the online article webpage). This could be due to the slight decomposition of **1c**. It is known that dimeric forms of benzoic acid derivatives exhibit liquid crystallinity [31]. In the present case, an introduction of two hydroxymethyl groups resulted in destabilisation of a mesophase formation due to the disturbance of the rotational fluctuations.

Table 1. Phase transition behaviours of **1**.

Acid	Phase transitions[a]
1a	heating Cr 155(29.4) Iso
	cooling Iso 103(–24.2) Cr
1b	heating Cr1 114(14.7) Cr2 131(21.2) Iso
	cooling Iso 116(–22.4) Cr2 99(–12.2) Cr1
1c	heating Cr1 122(21.3) Cr2 132(22.8) SmA 135/(1.0) Iso
	cooling Iso 134(–1.2) SmA 110(–23.4) Cr2[b] 96(–20.4) Cr1

[a] Transition temperatures (°C) and the corresponding enthalpies (in parentheses, kJmol^{-1}) were determined by differential scanning calorimety on the second heating and the second cooling (rate: 5°C min^{-1}). Cr, Sm A, and Iso indicate crystal, smectic A and isotropic liquid phases, respectively. Cr1, Cr2, and Cr3 indicate crystal phases. [b] Including some phase transitions between crystals.

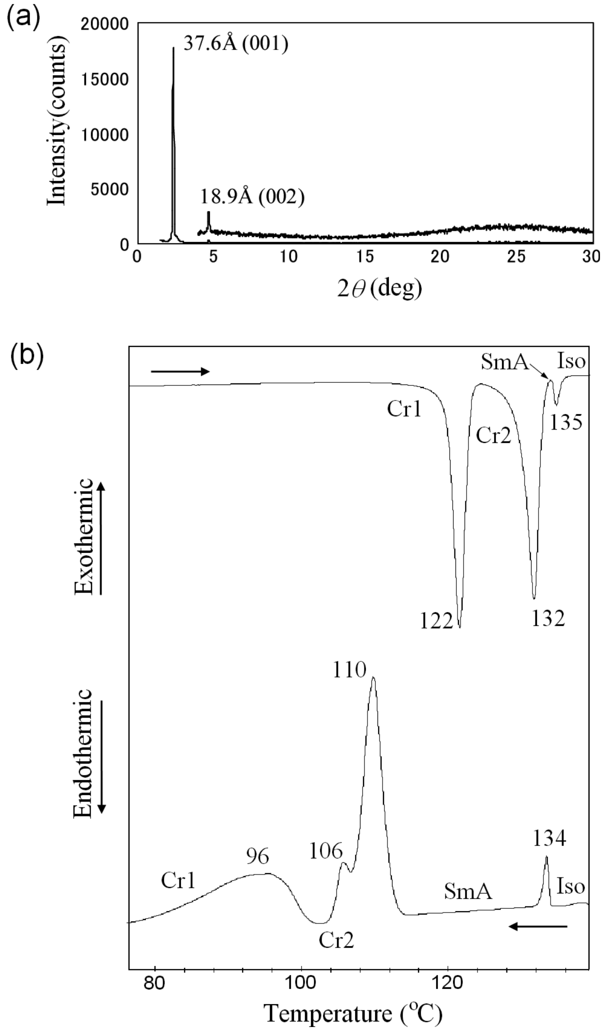

Figure 2. The X-ray diffraction pattern of **1c** at 134°C (a) and differential scanning calorimetry diagram of **1c** on the second heating (b) and the second cooling (c) with a heating and a cooling rate of 5°Cmin^{-1}, respectively.

3.2 Liquid crystallinity of 1 with one equivalent amount of alkylamine

Since the benzoic acids **1** did not give stable liquid crystals, we decided to introduce an ionic moiety to the core part to reinforce the core–core interaction. This will contribute to the formation of a well micro-phase-separated structure. It is known that amine salts of carboxylic acids [29, 32, 33] and sulphonic acids [34] form supramolecular liquid crystalline materials. However, in the former case, to the best of our knowledge, there is no report on the formation of the supramolecular liquid crystalline phases of the salts derived from monoamines and carboxylic acids. As a reference experiment, we checked the phase behaviour of the salt (1:1 mixture) of 4-dodecyloxybenzoic acid and octadecylamine. The salt did not show liquid crystallinity. However, the addition of monoamines possessing long alkyl chains to **1** promoted the formation of liquid crystal phases, as shown in Table 2.

The salt was prepared by dissolving **1** and alkylamine in THF in a ratio of 1:1 followed by evaporation of the solvent. All salts derived from **1b** and **1c** showed enantiotropic SmA phases. As an exception, the salt of **1a** with dodecylamine did not show a liquid crystal phase. The balance between the alkyl chain length of **1** and monoamine was the key factor in generating liquid crystal phases. In the series of salts of **1b** and **1c**, the enthalpy of the transition from the SmA phase to the isotropic phase became larger as the length of alkylamine became shorter. The flexibility of the alkyl chain caused a decrease in the transition enthalpy. It is important to have enough segregation of hydrogen-bonding parts from alkyl hydrophobic parts for the generation of the stable mesophase. Since the salts were oriented in the perpendicular direction on a glass plate, the dark field was observed in POM. Figure 3(a) shows the POM photograph of **1c**·$C_{16}H_{33}NH_2$ as an example. Similar patterns were observed for the other salts. The XRD image of the salts showed a typical diffraction pattern of a SmA phase. The XRD pattern of **1b**· $C_{16}H_{33}NH_2$ is presented in Figure 3(b) as a representative example. Three reflections in the small-angle region with *d*-spacings of 32.0 (001), 16.1 (002), 10.7 Å (003) indicated a well-defined periodic layer structure.

In addition, a broad halo was observed in the wide-angle region around 4.5 Å. The observed layer distance of the SmA phase by XRD was shorter than the calculated length of the salt. The interdigitation of alkyl chains occurred. In some cases, phase transitions among crystal phases were observed. Figure 4 shows DSC diagrams of the salts of **1b** with one equivalent amount of octadecylamine on the second heating and the second cooling.

In the first heating and cooling, phase transitions occurred at slightly higher temperature than those of the second heating and cooling. After the second heating–cooling cycle, they appeared almost at the same temperatures (see supplementary material Figure S2). Firstly, it is required to melt the mixture of the acid and the amine for the formation of homogenous salt. Consequently, steady phase transitions were observed after the second heating–cooling cycle. Three phase transitions among crystal phases were observed before the phase transition to a SmA phase on heating. There was a tendency that the layer distances of the SmA phase of the salts of **1** with alkylamines became shorter as the temperature increased (Table 3). For example, for the salt of **1b** and octadecylamine the observed layer distances were 34.2 and 31.7 Å at 90 and

Table 2. Phase transition behaviours of the salts of **1** with alkylamines.

Salt	Phase transitions[a]
1a· $C_{12}H_{25}NH_2$	heating Cr1 44(–16.2) Cr2 89(35.3) Iso cooling Iso 78(–0.7) Cr3 58(–3.9) Cr1
1a· $C_{14}H_{29}NH_2$	heating G 41(–36.0) Cr 79(29.4) SmA 103(1.1) Iso cooling Iso 101(–1.3) SmA 37(–2.8) G
1a· $C_{16}H_{33}NH_2$	heating G 64(–6.9) Cr 76(9.2) SmA 110(1.7) Iso cooling Iso 108(–1.6) SmA ND[b] G
1a· $C_{18}H_{37}NH_2$	heating Cr1 22(8.6) Cr2 78(13.6) SmA 122(1.0) Iso cooling Iso 120(–1.0) SmA 7(–5.6) Cr1
1b· $C_{12}H_{25}NH_2$	heating Cr1 10(0.7) Cr2 75(15.6) SmA 123(2.7) Iso cooling Iso 121(–2.7) SmA 18(–5.3) Cr1
1b· $C_{14}H_{29}NH_2$	heating G 14(2.6) Cr 78(10.1) SmA 127(1.5) Iso cooling Iso 126(–1.3) SmA 26(–10.0) G
1b· $C_{16}H_{33}NH_2$	heating G 12(6.9) Cr 79(22.1) SmA 126(1.5) Iso cooling Iso 123(–1.3) SmA 15(–8.0) G
1b· $C_{18}H_{37}NH_2$	heating Cr1 22(5.6) Cr2 43(–28.4) Cr3 57(8.9) Cr4 82(22.6) SmA 127(1.3) Iso cooling Iso 125(–1.3) SmA 20(–11.3) Cr1
1c· $C_{12}H_{25}NH_2$	heating Cr 86(56.7) SmA 121(2.2) Iso cooling Iso 119(–1.9) SmA 61(–38.2) Cr
1c· $C_{14}H_{29}NH_2$	heating Cr1 55(5.4) Cr2 83(40.6) SmA 122(1.5) Iso cooling Iso 122(–1.3) SmA 53(–58.3) Cr1
1c· $C_{16}H_{33}NH_2$	heating Cr1 75(13.6) Cr2 89(21.0) SmA 125(1.0) Iso cooling Iso 123(–1.0) SmA 61(–38.1) Cr1
1c· $C_{18}H_{37}NH_2$	heating Cr1 56(4.9) Cr2 87(64.3) SmA 120(0.8) Iso cooling Iso 119(–0.8) SmA 63(–79.0) Cr1

[a] Transition temperatures (°C) and the corresponding enthalpies (in parentheses, $kJmol^{-1}$) were determined by differential scanning calorimetry on the second heating and the second cooling (rate: $5°Cmin^{-1}$). Cr1, Cr2, Cr3, and Cr4, SmA, and Iso indicate crystal, smectic A and isotropic liquid phases, respectively. G indicates a glassy state.
[b] Not detected.

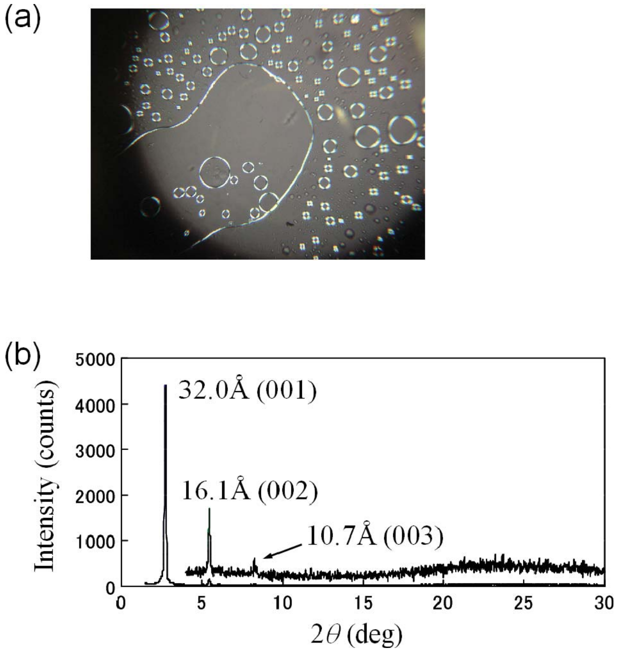

Figure 3. Polarising optical microscopy micrograph of the smectic A phase of **1c** with one equivalent amount of hexadecylamine at 105°C (a) and the X-ray diffraction pattern of **1b** with one equivalent amount of hexadecylamine at 90°C (b).

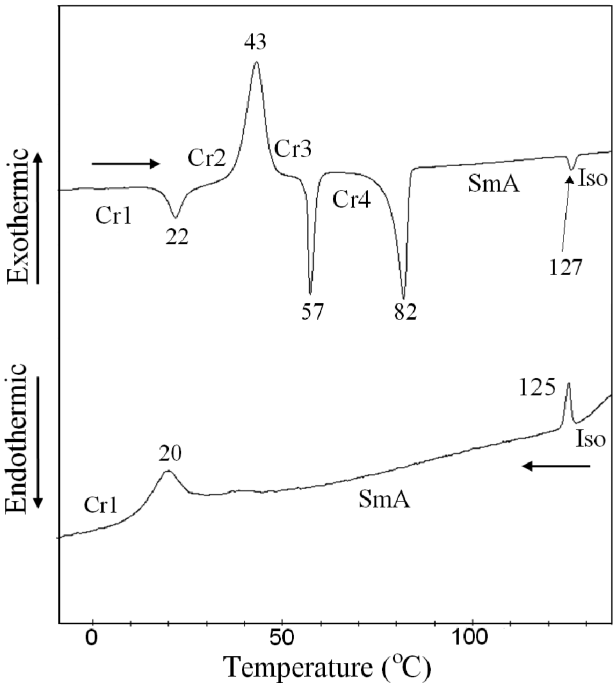

Figure 4. Differential scanning calorimetry diagram of **1b** with one equivalent amount of octadecylamine on the second heating (a) and the second cooling (b) with a heating and a cooling rate of $5°Cmin^{-1}$, respectively.

Table 3. Temperature dependent layer distances of SmA phases generated by a 1:1 mixture of **1** with alkylamine.

Salt	Temperature (°C)	Layer distance (Å)	Calculated length of salt (Å)
1a· $C_{14}H_{29}NH_2$	80	26.0	33.4
	90	25.8	
1a· $C_{16}H_{33}NH_2$	80	28.1	35.9
	90	27.9	
	100	27.6	
a· $C_{18}H_{37}NH_2$	80	29.9	38.4
	90	29.8	
	100	29.4	
	110	29.2	
	120	28.9	
1b· $C_{12}H_{25}NH_2$	80	29.8	38.4
	90	29.6	
	100	29.6	
	110	29.6	
1b· $C_{14}H_{29}NH_2$	90	31.1	40.9
	100	30.7	
	110	30.6	
	120	30.4	
1b· $C_{16}H_{33}NH_2$	90	32.0	43.4
	100	31.3	
	110	30.5	
	120	29.9	
1b· $C_{18}H_{37}NH_2$	90	34.2	45.9
	100	33.9	
	110	32.7	
	120	31.7	
1c· $C_{12}H_{25}NH_2$	90	32.9	45.9
	100	33.4	
	110	33.5	
	120	33.5	
1c· $C_{14}H_{29}NH_2$	90	34.2	48.4
	100	33.9	
	110	33.4	
	120	33.2	
1c· $C_{16}H_{33}NH_2$	90	37.3	50.9
	100	35.6	
	110	35.6	
	120	34.5	
1c· $C_{18}H_{37}NH_2$	90	38.7	53.4
	100	38.0	
	110	36.7	

120°C, respectively. They were shorter than the calculated length (45.9 Å) of the salt. The layer periodicities decreased as the temperature was increased. This is explained by the loss of the orientational order due to thermal fluctuations, leading to a stepwise destruction of the hydrogen bonds holding the molecules together.

Figure 5 shows the proposed layer structure of the 1:1 mixture of **1b** and dodecadecylamine. The hydrogen bonding along the molecular short axis aligns the salts, which results in a creation of a plough-shaped structure. Interdigitation of alkyl chains gives a layer structure. The ionic salt parts are segregated from the hydrophobic parts. This kind of alignment originating in the hydrogen bonding along the molecular short axes was reported by us in the crystal structure of the similar benzoic acid derivative [35].

3.3 The effect of the ratio of alkylamine on the liquid crystallinity

The phase transition behaviours of the mixture of **1b** and octadecylamine were investigated by varying their ratios (Figure 6). When the ratio of **1b** was low, **1b** and octadecylamine were not intermingled. When the ratio of **1b** was around 60–70%, a SmA phase was observed

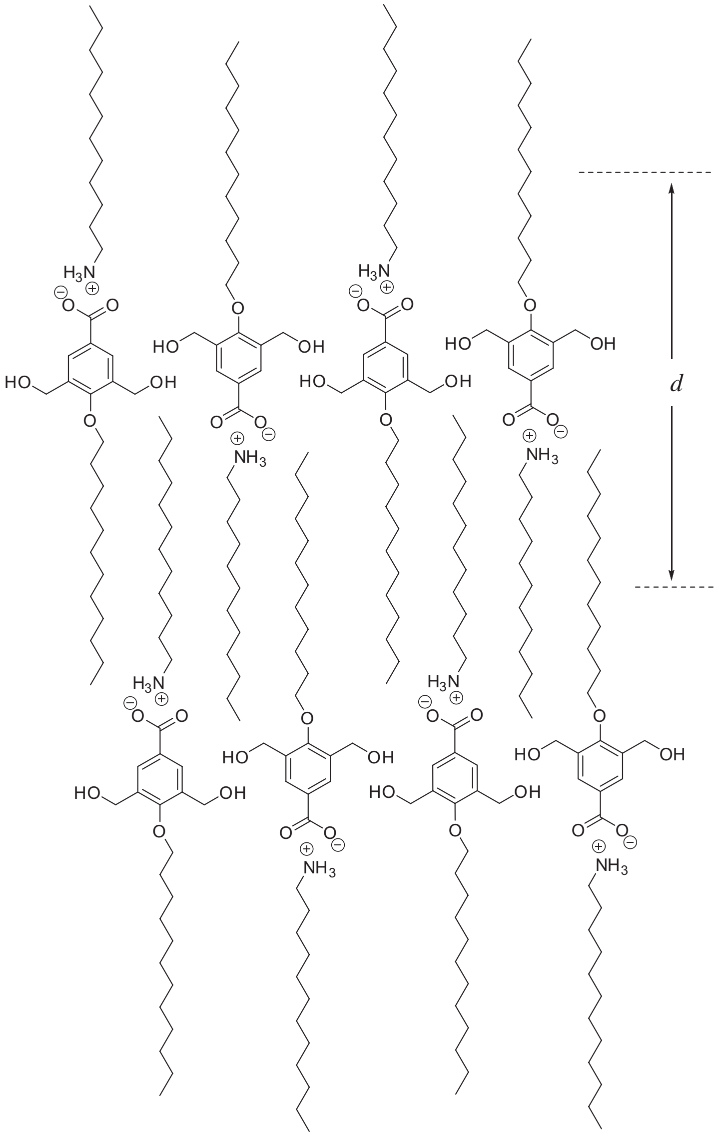

Figure 5. Proposed layer structure of **1b**· $C_{12}H_{25}NH_2$.

in a wide temperature range from an ambient temperature up to around 130°C.

In the case of the mixture with the ratio of 1:1, the $\nu_{C=O}$ of the corresponding salts was observed at around 1600 cm^{-1} (Figure 7(a)). No observation of $\nu_{C=O}$ around 1700 cm^{-1} indicated that the salts were formed completely. The mixture of **1b** and octadecylamine in a ratio of 2:1 showed two bands of $\nu_{C=O}$ at 1693 and 1603 cm^{-1} at 90°C (Figure 7(b)). The results indicated that the mixture contained two types of $\nu_{C=O}$. The former corresponded to the $\nu_{C=O}$ of the acid form and the latter agreed with that of the salt. From these results, we concluded that the 2:1 mixture of **1b** and octadecylamine consisted of the mixture of the salt of **1b** with octadecylamine and the dimeric form of **1b** in a ratio 2:1. Association of the dimeric form of **1c** with the salt merely lowered the phase transition temperature from the SmA phase to the crystal since the clearing points of the 1:1 and 2:1 mixtures of **1b** and octadecylamine were nearly the same (approximately 130°C).

4. Conclusion

In contrast to the general concept that disturbance of the rotational fluctuations of the core part of liquid crystal molecules destabilises their mesophases, the rod-like molecules **1** showed liquid crystallinity by salt formation with alkylamines. They possessed two hydrogen-bonding sites at the core toward the direction

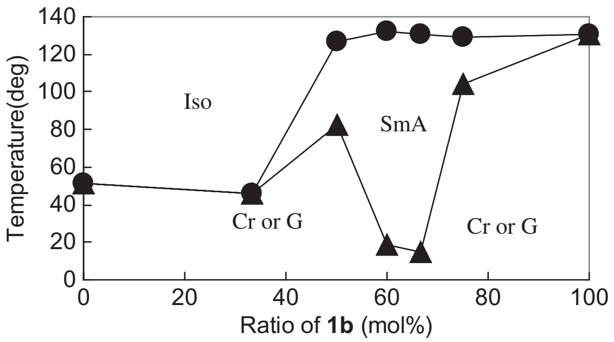

Figure 6. The acid–amine ratio-dependent phase transition diagram of the mixture of **1b** and octadecylamine.

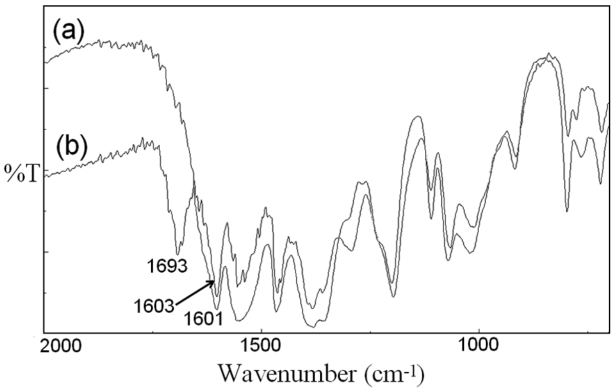

Figure 7. Infrared spectra of the salts of **1b** and octadecylamine in acid–amine ratios of 1:1(a) and 2:1(b).

of the molecular short axes; nevertheless, they showed stable mesophases. This hydrogen bonding will contribute to the efficient segregation between hydrogen-bonded ionic cores and alkyl chain parts. This is the key factor in stabilising the liquid crystal phases, which compensates for the instability caused by the obstruction of the rotational fluctuations. The difference of mesomorphism between the pure and amine salt of carboxylic acids originates in the ionic nature of the core. In the latter case, an efficient segregation between ionic cores and alkyl chain parts can be expected, which results in the formation of the stable mesophase.

References

[1] Lehn, J.-M. *Supramolecular Chemistry*; VCH: Weinheim, Germany, 1995.
[2] Desiraju, G.R. *Acc. Chem. Res.* **1996**, *29*, 441–449.
[3] Steed, J.W.; Atwood, J.L. *Supramolecular Chemistry*; John Wiley & Sons: Chichester, England, 2000.
[4] Fujita, M.; Umemoto, K.; Yoshizawa, M.; Fujita, N.; Kusukawa, T.; Biradha, K. *Chem. Commun.* **2001**, 509–518.
[5] Fitzmaurice, R.J.; Kyne, G.M.; Douheret, D.; Kilburn, J.D. *J. Chem. Soc. Perkin 1* **2002**, 841–864.
[6] Hofmeir, H.; Schubert, U.S. *Chem. Commun.* **2005**, 2423–2432.
[7] Binnemans, K. *Chem. Rev.* **2005**, *105*, 4148–4204.
[8] Kato, T.; Fréchet, J.M.J. *Am. Chem. Soc.* **1989**, *111*, 8533–8534.
[9] Kato, T.; Fujishima, A.; Fréchet, J.M.J. *Chem. Lett.* **1990**, 919–922.
[10] Kato, T.; Adachi, H.; Fujishima, A.; Fréchet, J.M.J. *Chem. Lett.* **1992**, 265–268.
[11] Paleos, C.M. *Mol. Cryst. Liq. Cryst.* **1994**, *243*, 159–183.
[12] Paleos, C.M.; Tsiourvas, D. *Liq. Cryst.* **2001**, *28*, 1127–1161.
[13] Kato, T.; Mizoshita, N.; Kishimoto, K. *Angew. Chem. Int. Ed.* **2006**, *45*, 38–68.
[14] Kato, T.; Kubota, Y.; Nakano, M.; Uryu, T. *Chem. Lett.* **1995**, 1127–1128.
[15] Kleppinger, R.; Lillya, C.P.; Yang, C. *Angew. Chem. Int. Ed. Engl.* **1995**, *34*, 1637–1638.
[16] Kraft, A.; Reichert, A.; Kleppinger, R. *Chem. Commun.* **2000**, 1015–1016.
[17] Joachimi, D.; Tschierske, C.; Müller, H.; Wendorff, J.H.; Schneider, L.; Kleppinger, R. *Angew. Chem. Int. Ed. Engl.* **1993**, *32*, 1165–1167.
[18] Kölbel, M.; Beyersdorff, T.; Cheng, X.H.; Tschierske, C.; Kain, J.; Diele, S. *J. Am. Chem. Soc.* **2001**, *123*, 6809–6818.
[19] Lehn, J.-M. *Polym. Int.* **2002**, *51*, 825–839.
[20] Lu, X.; He, C.; Griffin, A.C. *Macromolecules* **2003**, *36*, 5195–5200.
[21] Jeong, K-U.; Jin, S.; Ge, J.J.; Knapp, B.S.; Graham, M.J.; Ruan, J.; Guo, M.; Xiong, H.; Harris, F.W.; Cheng, S.Z.D. *Chem. Mater.* **2005**, *17*, 2852–2865.
[22] Xu, J.; Toh, C.L.; Liu, X.; Wang, S.; He, C.; Lu, X. *Macromolecules* **2005**, *38*, 1684–1690.
[23] Hildebrandt, F.; Schröter, A.; Tschierske, C.; Festag, R.; Kleppinger, R.; Wendorff, J.H. *Angew. Chem. Int. Ed. Engl.* **1995**, *34*, 1631–1633.
[24] Mori, A.; Nimura, R.; Takeshita, H. *Chem. Lett.* **1991**, 77–80.
[25] Mori, A.; Katahira, K.; Kida, K.; Takeshita, H. *Chem. Lett.* **1992**, 1767–1770.
[26] Kajitani, T.; Kohmoto, S.; Yamamoto, M.; Kishikawa, K. *Chem. Mater.* **2004**, *16*, 2329–2331.
[27] Kanie, K.; Yasuda, T.; Ujiie, S.; Kato, T. *Chem. Commun.* **2000**, 1899–1900.
[28] Ringsdorf, H.; Schlarb, B.; Venzmer, J. *Angew. Chem. Int. Ed. Engl.* **1998**, *27*, 113–158.
[29] Martín-Rapún, R.; Marcos, M.; Omenat, A.; Barberá, J.; Romero, P.; Serrano, J.L. *J. Am. Chem. Soc.* **2005**, *127*, 7397–7403.
[30] Mathevet, F.; Masson, P.; Nicoud, J.-F.; Skoulios, A. *J. Am. Chem. Soc.* **2005**, *127*, 9053–9061.
[31] Gray, G.W.; Jones, B. *J. Chem. Soc.* **1953**, 4179–4180.
[32] Ishida, Y.; Amano, S.; Saigo, K. *Chem. Commun.* **2003**, 2338–2339.
[33] Katoh, M.; Uehara, S.; Kohmoto, S.; Kishikawa, K. *Chem. Lett.* **2006**, 322–323.
[34] Ito, M.; Matsunaga, Y.; Matsuzaki, H.; Shimojima, S. *Bull. Chem. Soc. Jpn.* **1989**, *62*, 3919–3922.
[35] Kohmoto, S.; Kuroda, Y.; Someya, Y.; Kishikawa, K.; Masu, H.; Yamaguchi, K.; Azumaya, I. *Cryst. Growth Des.* **2009**, *9*, 3457–3462.